ARTICLE

PTPL1 suppresses lung cancer cell migration via inhibiting TGF-β1-induced activation of p38 MAPK and Smad 2/3 pathways and EMT

Ning Zhu[1], Xiu-juan Zhang[1], Hai Zou[1], Yuan-yuan Zhang[1], Jing-wen Xia[1], Peng Zhang[1], You-zhi Zhang[1], Jing Li[1], Liang Dong[1], Gulinuer Wumaier[1] and Sheng-qing Li[1]

Epithelial-mesenchymal transition (EMT) enables dissemination of neoplastic cells and onset of distal metastasis of primary tumors. However, the regulatory mechanisms of EMT by microenvironmental factors such as transforming growth factor-β (TGF-β) remain largely unresolved. Protein tyrosine phosphatase L1 (PTPL1) is a non-receptor protein tyrosine phosphatase that plays a suppressive role in tumorigenesis of diverse tissues. In this study we investigated the role of PTPL1/PTPN13 in metastasis of lung cancer and the signaling pathways regulated by PTPL1 in terms of EMT of non-small cell lung cancer (NSCLC) cells. We showed that the expression of PTPL1 was significantly downregulated in cancerous tissues of 23 patients with NSCLC compared with adjacent normal tissues. PTPL1 expression was positively correlated with overall survival of NSCLC patients. Then we treated A549 cells in vitro with TGF-β1 (10 ng/mL) and assessed EMT. We found that knockdown of PTPL1 enhanced the migration and invasion capabilities of A549 cells, through enhancing TGF-β1-induced EMT. In nude mice bearing A549 cell xenografts, knockdown of PTPL1 significantly promoted homing of cells and formation of tumor loci in the lungs. We further revealed that PTPL1 suppressed TGF-β-induced EMT by counteracting the activation of canonical Smad2/3 and non-canonical p38 MAPK signaling pathways. Using immunoprecipitation assay we demonstrated that PTPL1 could bind to p38 MAPK, suggesting that p38 MAPK might be a direct substrate of PTPL1. In conclusion, these results unravel novel mechanisms underlying the regulation of TGF-β signaling pathway, and have implications for prognostic assessment and targeted therapy of metastatic lung cancer.

Keywords: PTPL1; non-small cell lung cancer; migration and invasion; EMT; TGF-β1; p38MAPK; Smad2/3; SB203580

INTRODUCTION

Lung cancer is one of the most lethal malignancies worldwide [1]. Metastasis and recurrence are the main causes of death in lung cancer patients, accounting for nearly 90% of cancer-related deaths. Epithelial-to-mesenchymal transition (EMT) is considered to be a key impetus for the migration and invasion of neoplastic cells [2, 3]. EMT refers to the transformation of polarized epithelial cells into motile, nonpolarized stromal cells under specific physiological or pathological conditions, accompanied by decreased intercellular adhesion and contact, extracellular matrix remodeling, and increased cell motility [3–5]. In metastatic tumors, microenvironmental factors can elicit EMT by activating diverse signaling pathways [6, 7], notably, the transforming growth factor β (TGF-β) signaling pathway, a master regulator of EMT. TGF-β binds to a type II receptor dimer, which recruits a type I receptor dimer to form a heterotetrameric complex with the ligand [8]. During canonical signaling, receptor activation induces C-terminal phosphorylation of a group of transcription factors (TFs) called Smads to regulate gene expression [9]. During noncanonical signaling, TGF-β can activate downstream signaling pathways, such as the p38 MAPK, ERK1/2, and PI3K/AKT pathways [9–11]. The aforementioned pathways synergistically activate a class of transcription factors, including Snail1, Slug, ZEB1/2, and Twist1/2, which eventually downregulate epithelial cell markers such as E-cadherin and promote the expression of mesenchymal cell markers such as N-cadherin, vimentin, and α-SMA [11–13]. However, the role of the TGF-β signaling regulatory network in the metastasis of lung cancer is not fully understood.

Tyrosine phosphorylation is a key step in signal transduction and the regulation of enzymatic activity [14]. Thus, the balance between protein tyrosine phosphatases (PTPs) and protein tyrosine kinases (PTKs) plays essential roles in maintaining the homeostasis of intracellular signaling that controls various cell behaviors, such as division, morphogenesis, and motility. Protein tyrosine phosphatase L1 (PTPL1) is a nonreceptor protein tyrosine phosphatase also called PTPN13, FAP-1, PTP-BAS, and PTP1E [15]. The human *PTPL1* gene is mapped to chromosome 4q21.3 and encodes a 270 kDa protein mainly distributed on the inner surface of the cytoplasmic membrane [15]. The PTPL1 protein contains a KIND domain, a FERM region, 5 PDZ motifs, and a highly conserved PTP catalytic region [15]. The regional function of the KIND domain is still unclear. The PDZ motifs can bind to and catalyze the dephosphorylation of different proteins, thereby participating in the regulation of different

[1]Department of Pulmonary and Critical Care Medicine, Huashan Hospital, Fudan University, Shanghai 200040, China
Correspondence: Sheng-qing Li (shengqingli@hotmail.com)
These authors contributed equally: Ning Zhu, Xiu-juan Zhang.

PTPL1 inhibits lung cancer metastasis via P38 MAPK
N Zhu et al.

1281

cellular processes as well as the occurrence of various diseases [16–18]. PTPL1 was first identified to inhibit apoptosis as an interacting partner of the death receptor [19], and further studies found that PTPL1 promotes Wnt signaling by stabilizing β-catenin [20]. However, accumulating evidence indicates that PTPL1 plays a suppressive role in tumorigenesis in diverse tissues [21, 22]. The PTPL1 gene harbors mutations or is significantly downregulated in colon cancer, liver cancer, breast cancer, and head and neck cancer [23, 24]. Scrima M et al. found that PTPL1 deficiency was critically involved in the development of non-small cell lung cancer (NSCLC) [25]. We previously found that PTPL1 dephosphorylates Src kinase and that PTPL1 downregulation underlies the decrease in the sensitivity of NSCLC to tyrosine kinase inhibitors targeting epithelial growth factor receptors (EGFR-TKIs) [26]. Here, we explored the role of PTPL1 in the metastasis of lung cancer and investigated the molecular pathways regulated by PTPL1 that affect EMT in lung cancer cells.

MATERIALS AND METHODS

Patients
Lung adenocarcinoma patients confirmed by surgical pathology were enrolled. Lung adenocarcinoma tissues and corresponding adjacent normal tissues were collected. All patients signed informed consent forms, and all experimental procedures were approved by the Ethics Committee of Fudan University, China (Permit Number: KY2016-396).

Quantitative RT-PCR
Total RNA was extracted from cells using TRIzol reagent (Invitrogen, Carlsbad, CA) according to the manufacturer's protocol. Reverse transcription was performed using SuperScript™ II Reverse Transcriptase (Invitrogen), and cDNA was amplified and detected using SYBR® Premix Ex Taq™ (TaKaRa, Kusatsu, Shiga, Japan). The PCR primer sequences were designed as follows— GAPDH-F: 5′-TGCACCACCAACTGCTTAGC-3′, GAPDH-R: 5′-GGCATG GACTGTGGTCATGAG-3′; PTPL1-F, 5′-TGGCTCTCCAGGCTGAGTAT G-3′, PTPL1-R: 5′-AACACCAAACAAAATGGTCCTG-3′. E-Cadherin-F: 5′-AGAACGCATTGCCACATACACTC-3′, E-Cadherin-R: 5′-CATTCTGA TCGGTTACCGTGATC-3′; N-Cadherin-F: 5′-CAAGATGGGTCAATGG AAATAG-3′, N-Cadherin-R: 5′-CTCAGGAATACGAGCCTTCAC-3′; Slug-F: 5′-ACACATTACCTTGTGTTTGCAAGATCT-3′, Slug-R: 5′- TGTC TGCAAATGCTCTGTTGCAGTG-3′; Snail-F: 5′-CCTCAAGATGCACAT CCGAAGCCAC-3′, Snail-R: 5′-CCGGACATGGCCTTGTAGCAGC-3′. This experiment used 10 μl reaction systems, and the following groups of PCR mixtures (preparation of the reaction liquid mixtures needs to be performed on ice) were prepared to record the peak Ct of each well, as follows: $Ct = Ct_{gene} - Ct_{Internal\ reference}$; $\Delta\Delta Ct = \Delta Ct_{experimental\ group} - \Delta Ct_{control\ group}$; relative mRNA expression level in each sample = $2^{-\Delta\Delta Ct}$.

Western blot
Samples of protein lysate were loaded in SDS-PAGE gels in electrophoresis tanks with the appropriate buffer concentration; 40-μg protein samples were loaded in each lane. Running buffer was added, and electrophoresis was performed at 90 V for 20 min. After each sample was separated in a straight line, the gel was electrophoresed at 120 V until the bromophenol blue band was near the bottom of the gel (approximately 60 min). Proteins were transferred to an NC membrane at 500 mA for 90 min. A 5% milk solution was prepared in 1×PBST and sealed for 1 h. Then, a working solution containing the primary antibody was added and incubated overnight on a shaker table at 4 °C. The primary antibodies used for immunoblotting were as follows: anti-PTPL1 (Novus, IMG-5726), anti-E-cadherin (CST, #14472), anti-N-cadherin (CST, #13116), anti-Smad2/3 (CST, #3102), anti-phospho-Smad2/3 (CST, #8828), anti-p38MAPK (CST, #9212), anti-phospho-p38MAPK (CST, #9216), anti-Snail1 (CST, #3879), anti-Slug (CST, #9585), and anti-GAPDH (CST, #2118). The

membrane was rinsed 4 times with 1×PBST and incubated in the corresponding working solution containing the secondary antibody in a shaker at room temperature for 1 h. The secondary antibody working solution was discarded, and the target strip was rinsed 4 times with 1×PBST for 5 min each time. Immunoreactions were visualized via incubation in ECL chemiluminescence reagent (Amersham Life Science, Arlington Heights, USA), and the membrane was scanned using an Odyssey Imaging System (LI-COR, Lincoln, USA).

Gene knockdown
Short hairpin RNAs (shRNAs) against PTPL1 and a scrambled shRNA sequence were expressed from the lentiviral vector pGreen-Puro (System Biosciences). The following shRNA oligos were designed and synthesized: PTPL1-1 sense, 5′-GATCCCCTTTGGATCAGTGTCT AATTTTCAAGAGAAATTAGACACTGATCCAAAGGTTTTTG-3′; PTPL1-1 anti-sense, 5′-AATTCAAAAACCTTTGGATCAGTGTCTAATTTCTCTTGAA AATTAGACACTGATCCAAAGGG-3′; PTPL1-2 sense: 5′- GATCCGCC ACGGTCTATTCTTACTAATTCAAGAGATTAGTAAGAATAGACCGTGGCT TTTTG-3′; PTPL1-2 anti-sense: 5′-AATTCAAAAAGCCACGGTCTATTCT TACTAATCTCTTGAATTAGTAAGAATAGACCGTGGCG-3′. The paired oligos were annealed and cloned into the vector prior to lentiviral packaging according to the manufacturer's protocol.

Wound healing assay
Tumor cells were incubated in complete medium in an incubator at 37 °C and 5% CO_2 until they adhered to and fully contacted the dishes. Complete medium was replaced with serum-free medium, and cells were starved for 24 h. Scratches were made with a sterile 200 μL pipette tip. The tip was held perpendicular to the bottom of the plate. The scratches were made perpendicular to the labeling lines on the Petri dish. The scratches were observed and photographed under an inverted microscope at 0 h and 24 h, and the healing of the scratches was evaluated. The scratch widths were measured, and the data were analyzed.

Transwell assay
Cells in logarithmic phase were harvested, and a suspension with a concentration of 5×10^6 cells/200 μl was prepared. Transwell chamber inserts were placed in a 24-well plate, 800 μL of complete culture medium was added to the lower chambers, and 200 μL of cell suspension in serum-free culture medium was added to the upper chambers. The plates were incubated in an incubator at 37 °C and 5% CO_2 for 24 h. The chambers were then removed, cells were gently wiped from the upper chambers, and the chambers were rinsed with PBS three times. Cells were immobilized with anhydrous methanol for 30 min, stained with 0.5% crystal violet for 30 min, and rinsed with PBS three times. The number of invaded cells in each field of view was counted, and the average number was recorded.

Immunohistochemistry
Lung cancer and adjacent tissue specimens were collected and fixed with 10% formalin for more than 24 h. Paraffin-embedded tissue sections were dewaxed, incubated at room temperature with 3% H_2O_2 for 10 min, washed with distilled water and immersed in PBS two times for 5 min each. Sections were blocked using 10% goat serum (PBS diluted) and incubated with the primary antibody (anti-E-cadherin, CST) prior to incubation with a horseradish peroxidase-conjugated secondary antibody. Sections were counterstained with hematoxylin, dehydrated in a graded ethanol series, and cleared with xylene.

Immunoprecipitation
Cell lysates were prepared in lysis buffer [50 mM Tris-HCl (pH 7.4), 150 mM NaCl, 20 mM EDTA, 50 mM NaF, 0.5% NP-40, 0.1 mM Na_3VO_4, 1 mM leupeptin, 20 mg/mL aprotinin, 1 mM dithiothreitol, and 1 mM PMSF]. Lysates (500 mL) were then incubated overnight at 4 °C with 5 μg of antibodies (anti-PTPL1, Novus; anti-p38 MAPK;

PTPL1 inhibits lung cancer metastasis via P38 MAPK
N Zhu et al.

1282

CST) and 25 μL of Dynabeads® Protein G (Novex, Thermo Fisher). The beads were washed three times with 1 mL of lysis buffer before boiling in sample buffer prior to Western blot analysis.

Experimental lung metastasis assay
Eight BALB/c nude mice aged 3 weeks were divided into two groups. The Ubi-MCS-firefly Luciferase-IRES-Puromycin plasmid (Biovector, Beijing, China) was transfected into control and PTPL1 knockdown A549 cells. Mice were then injected with these cells via the caudal vein. The body weights of the nude mice were monitored every 5 days for 6 weeks. After intraperitoneal anesthesia with chloral hydrate, D-fluorescein potassium salt (working concentration 15 mg/ml, 10 μL/g fluorescein/body weight) was injected intraperitoneally. Bioluminescence imaging was conducted with a Xenogen IVIS Kinetic imaging system, and the bioluminescence intensities were calculated. The care of the mice was in accordance with institutional guidelines.

Statistical analysis
GraphPad Prism 6.0 software was used for statistical analysis of data, and ImageJ software was used for grayscale scanning. Data are expressed as the mean ± SEM values. Data were compared between two groups by a t-test, and data were compared among multiple groups by analysis of variance. * $P < 0.05$, **$P < 0.01$, ***$P < 0.001$, and ****$P < 0.0001$.

RESULTS
PTPL1 expression correlates with the prognosis of NSCLC patients
We used data sets in The Cancer Genome Atlas (TCGA) to analyze the expression of PTPL1 in NSCLC patients and found that PTPL1 mRNA levels in cancer tissues were much lower than those in normal lung tissues (Fig. 1a). Quantitative RT-PCR and immuno-histochemical staining analyses of NSCLC specimens showed that PTPL1 was significantly downregulated in lung adenocarcinoma tissues compared with paired adjacent normal tissues (Fig. 1b, c).

PTPL1 levels in NSCLC cell lines were markedly lower than those in an immortalized bronchial epithelial cell line, BEAS-2B, as determined by RT-PCR and Western blot analyses (Fig. 1d, e). The relationship of PTPL1 expression with the prognosis of NSCLC patients was next investigated based on the Kaplan-Meier plotter online database. The PTPL1 level was found to be positively correlated with overall survival (OS) in NSCLC (HR = 0.74, 95% CI: 0.65, 0.84, $P < 0.01$) (Fig. 1f). A higher PTPL1 level predicted a better patient outcome in lung adenocarcinoma (HR = 0.49, 95% CI: 0.39, 0.63, $P < 0.01$) (Fig. 1g). Subgroup analysis showed that a high PTPL1 levels were associated with prolonged OS in both male and female NSCLC patients (Table 1). In terms of smoking, higher PTPL1 levels correlated with significantly longer OS times in lung

Table 1. Subgroup analysis of PTPL1 expression and overall survival time of lung cancer patients.

|	Patient number		HR	P
	High expression	Low expression		
Histology type				
NSCLC	963	963	0.74(0.65–0.84)	<0.05
Adenocarcima	358	362	0.49(0.39–0.63)	<0.05
Squamous	262	262	1(0.79–1.27)	0.99
Gender				
Male	549	551	0.81(0.69–0.95)	<0.05
Female	357	358	0.65(0.52–0.82)	<0.05
Smoking				
Smoking/Ever	249	250	0.77(0.59–1.01)	0.054
Never smoking	103	102	0.35(0.19–0.65)	<0.05
Stage				
Stage 1	185	185	0.4(0.26–0.6)	<0.05
Stage 2	68	68	0.48(0.29–0.78)	<0.05
Stage 3	12	12	0.27(0.09–0.83)	<0.05
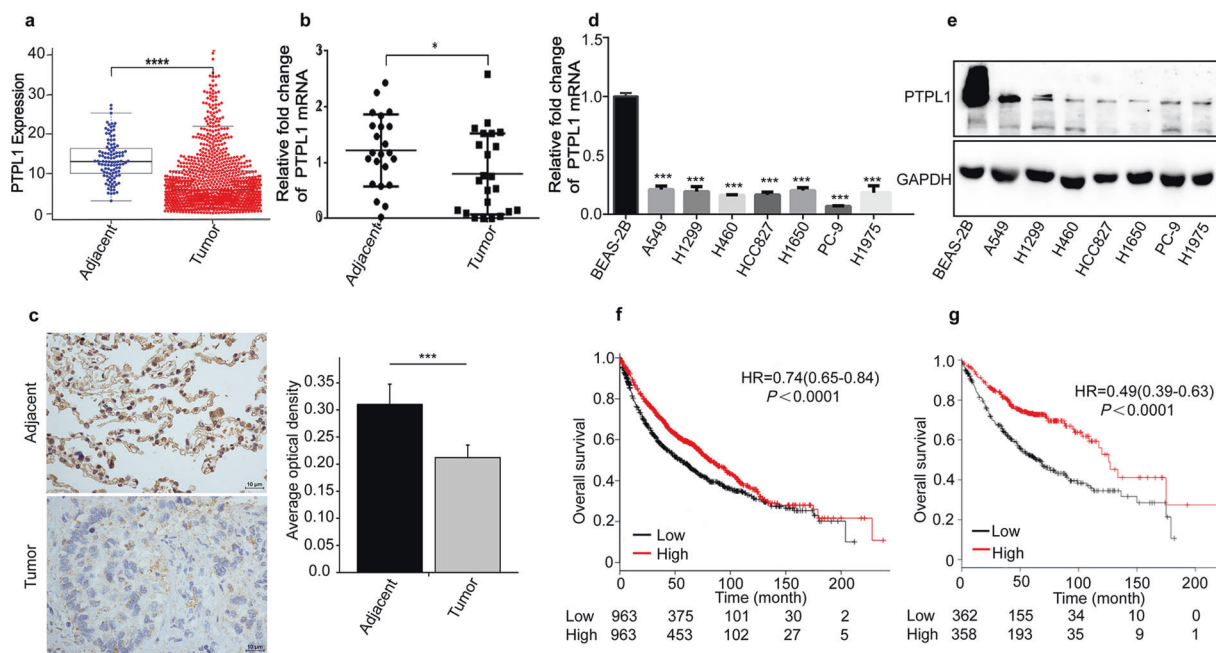
Fig. 1 PTPL1 is associated with the occurrence and prognosis of NSCLC. a Data of PTPL1 expression in clinical NSCLC and normal lung tissues were extracted from TCGA database and used for plotting. Specimens including 23 lung cancer tissues and paired adjacent normal tissues were used for qRT-PCR assay (**b**) and immunohistochemically staining (**c**) for PTPL1 (each bar represents the mean ± SEM. *$P < 0.05$, ***$P < 0.001$, ****$P < 0.0001$). Real-time PCR (**d**) and Western blot (**e**) were used to detect the expression of PTPL1 NSCLC cell lines and a normal alveolar epithelial cell line, BEAS-2B (each bar represents the mean ± SEM. ***$P < 0.001$ vs. BEAS-2B). **f, g** TCGA data were used for analysis of correlation of PTPL1 with overall survival (OS) of all NSCLC patients (**f**), patients with lung adenocarcinoma (**g**).
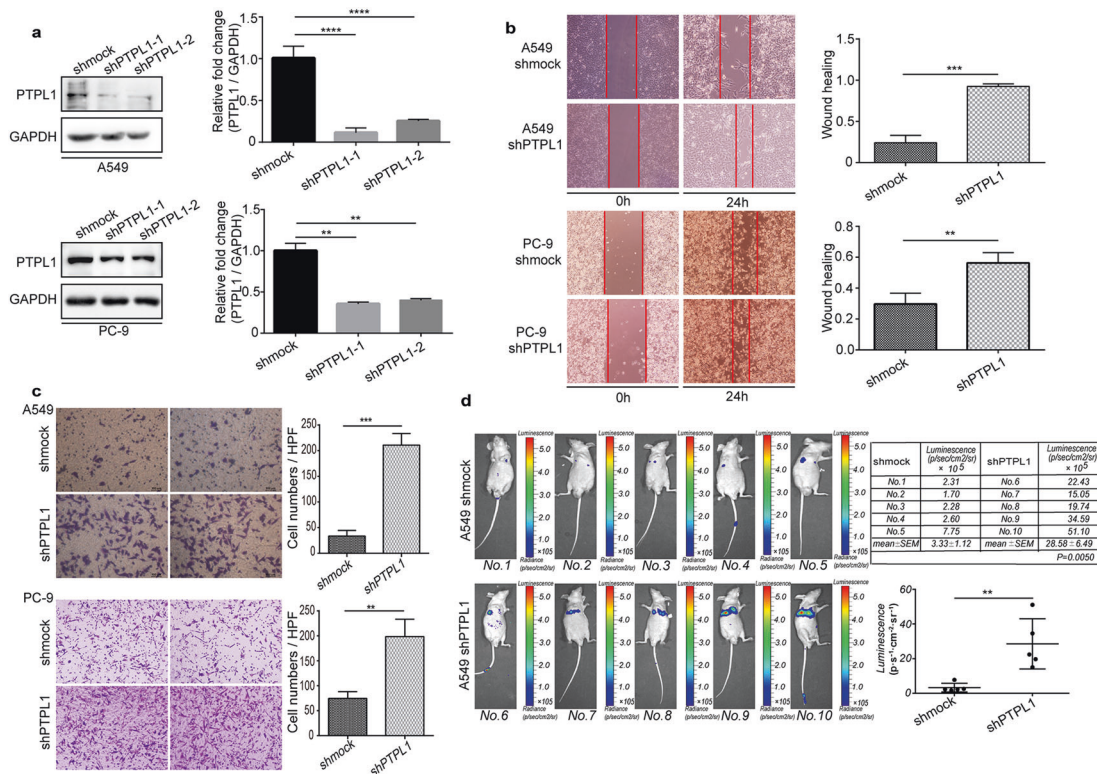
PTPL1 inhibits lung cancer metastasis via P38 MAPK
N Zhu et al.

1283

Fig. 2 PTPL1 knockdown promotes migration and invasion of NSCLC cells. a A549 cells were infected by lentiviruses without an shRNA-expressing cassette (shmock) or those expressing shRNAs targeting PTPL1, followed by Western blot analysis of the cell lysates (each bar represents the mean ± SEM. **$P < 0.01$, ****$P < 0.0001$ vs. the shmock group). Wound healing assay (**b**) and Transwell assay for cell invasion (**c**) using A549 cells or PC-9 cells infected by lentiviruses described in (**a**) (each bar represents the mean ± SEM. **$P < 0.01$, ***$P < 0.001$ vs. the shmock group). **d** BALB-c nude mice were injected via caudal vein with luciferase-expressing A549 cells with or without PTPL1 knockdown. Bioluminescence was imaged on a Xenogen IVIS Kinetic imaging system, and the bioluminescence intensities were calculated and plotted (each bar represents the mean ± SEM. **$P < 0.01$ vs. the shmock group).

cancer patients without a smoking history but not in smokers or former smokers (Table 1). When patients were stratified by stage, higher PTPL1 levels were correlated with significantly longer OS times in lung cancer patients, regardless of stage. Furthermore, the earlier the stage, the greater was the survival benefit in patients with high PTPL1 expression. Thus, PTPL1 is a prognostic factor whose high expression correlates with prolonged OS in NSCLC patients.

PTPL1 suppresses the migration and invasion of NSCLC cells
We next investigated the regulatory role of PTPL1 in the malignant phenotypes of NSCLC cells. PTPL1 was knocked down in NSCLC cell lines via lentivirus-delivered shRNAs (Fig. 2a). Wound healing assays showed that knockdown of PTPL1 enhanced the migration capability of NSCLC cells (Fig. 2b), and Transwell assays indicated that the invasive capacity of NSCLC cells was substantially increased after PTPL1 silencing (Fig. 2c). The migration and invasion abilities of NSCLC cells were next evaluated in vivo by injection of luciferase-expressing A549 cells via the caudal vein. We found that knockdown of PTPL1 significantly promoted homing of cells and formation of tumor loci in the lungs (Fig. 2d). These results suggest that PTPL1 plays an inhibitory role in the migration and invasion of NSCLC cells.

PTPL1 impairs NSCLC cell invasion via suppression of EMT
EMT has been documented as a key driver of cancer metastasis. We then investigated whether PTPL1 represses the migration and invasion of NSCLC cells by impairing EMT. Indeed, in both A549 and PC-9 cells, knockdown of PTPL1 triggered a marked morphological change characterized by loss of cell adhesion and

polarity (Fig. 3a). Consistent with this result, PTPL1 knockdown reduced the expression of the epithelial marker E-cadherin, as evidenced by immunofluorescence staining (Fig. 3b). Further, PTPL1 knockdown in lung cancer cells significantly enhanced TGF-β1-induced downregulation of E-cadherin and upregulation of N-cadherin (Fig. 3c, d). These data suggest that PTPL1 impedes EMT in NSCLC cells induced by the microenvironmental factor TGF-β1.

PTPL1 suppresses EMT by inhibiting noncanonical TGF-β pathways
The occurrence of EMT is characterized by a prominent transition in gene expression profiles induced by a class of transcription factors (TFs), e.g., Snail1 and Snail2/Slug. We thus sought to determine whether PTPL1 regulates the expression of these TFs in NSCLC cells. We found that the increases in the mRNA or protein expression levels of Snail1 and Slug induced by TGF-β1 were further elevated upon knockdown of PTPL1 (Fig. 4a, b). Then, we explored the effect of PTPL1 expression on the canonical and noncanonical TGF-β1/TβRII signaling pathways. Consistent with the above finding, we found that PTPL1 silencing facilitated TGF-β-induced activation of Smad2/3 (Fig. 4c) and p38 MAPK (Fig. 4d). Therefore, PTPL1 represses TGF-β-induced EMT by counteracting the activation of canonical Smad2/3 and noncanonical p38 MAPK signaling pathways in NSCLC cells.

PTPL1 impairs TGF-β signaling and EMT by targeting p38 MAPK
In this study, we focused on exploring how PTPL1 represses noncanonical TGF-β/TβRII signaling in NSCLC cells. Immunoprecipitation assays showed that PTPL1 can bind to p38 MAPK (Fig. 5a), suggesting that p38 MAPK is a direct substrate of the tyrosine phosphatase PTPL1. In addition, inhibition of p38 MAPK by
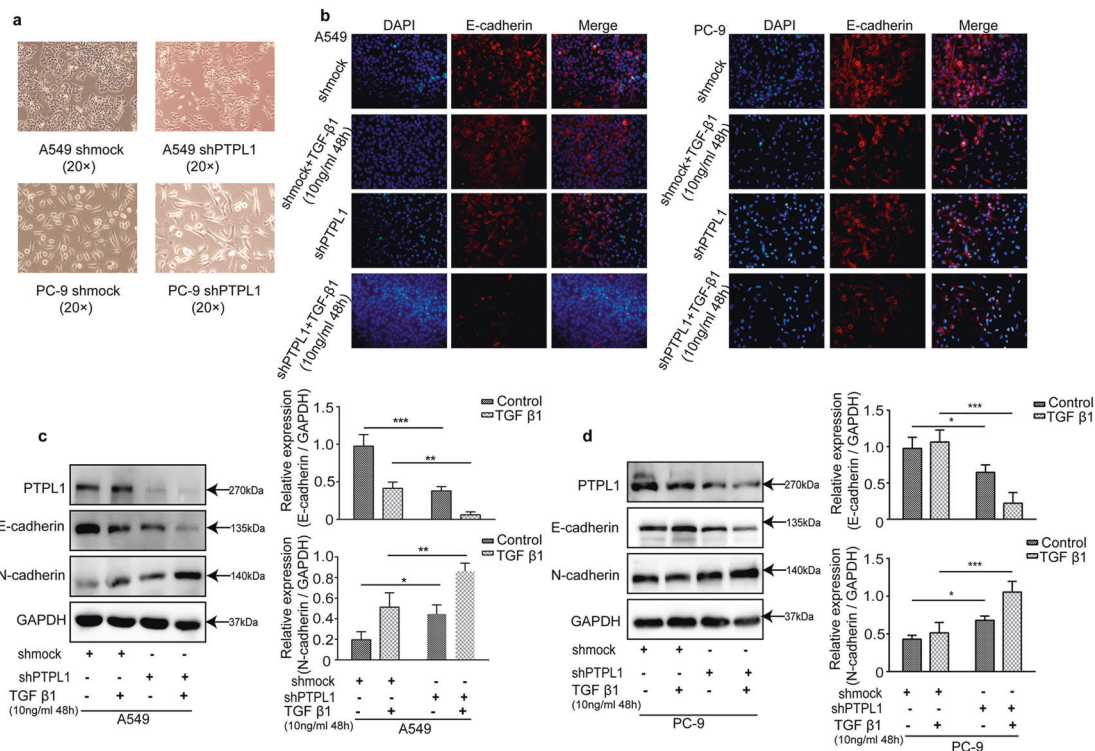
PTPL1 inhibits lung cancer metastasis via P38 MAPK
N Zhu et al.

1284

Fig. 3 PTPL1 knockdown facilitates EMT of NSCLC cells. a, b NSCLC cells were infected by lenviruses without an shRNA-expressing cassette (shmock) or those expressing PTPL1-targeted shRNA, and were observed under inverted microscope (**a**) and subject to immunofluorescent staining for indicated proteins (**b**). **c, d** Cells in (**a**) were further treated with or without TGF-β1, and were subject to Western blot analysis (each bar represents the mean ± SEM. *$P < 0.05$, **$P < 0.01$, ***$P < 0.001$ vs. the shmock group).

SB203580 attenuated the increase in the invasive capacity of TGF-β-treated NSCLC cells in a Transwell assay (Fig. 5b). Moreover, the morphological change caused by PTPL1 knockdown was partially reversed by SB203580 (Fig. 5c). PTPL1-mediated dephosphorylation of proteins in the TGF-β pathway negatively regulates EMT, because a p38 MAPK inhibitor counteracted the changes in EMT markers and TFs induced by PTPL1 silencing (Fig. 5d, e). Taken together, these data suggest that PTPL1 suppresses NSCLC cell EMT and invasion by dephosphorylating p38 MAPK.

DISCUSSION

Malignant cells and educated cells in the microenvironment release an abundance of inflammatory factors or growth factors to support tumor progression and distal metastasis. These factors play essential roles in the induction of EMT, a hallmark of highly aggressive solid tumors. In particular, TGF-β has been documented as a pivotal driver of EMT, participating in canonical signaling via the Smad transcription factor family and noncanonical signaling through activation of the PI3K/Akt and Ras/MAPK pathways [27, 28]. However, the mechanisms through which TGF-β signaling and EMT are regulated in NSCLC cells remain to be fully understood. We established here that the protein tyrosine phosphatase PTPL1 impairs EMT in NSCLC cells by targeting both TGF-β signaling pathways (Fig. 5f) and that PTPL1 deficiency is associated with poor prognosis in NSCLC patients. These findings highlight the critical involvement of homeostasis between protein tyrosine kinases and phosphatases in regulating classical intracellular pathways and preventing the occurrence and progression of malignancies.

The nonreceptor protein tyrosine phosphatase (PTPN) family consists of 17 members, each containing a highly conserved catalytic region and a series of functional regulatory regions.

Accumulating evidence has shown that these PTPNs play essential roles in carcinogenesis in various tissues [17, 29–31]. However, PTPNs might function as either tumor suppressors or oncoproteins depending on their interacting partners and dephosphorylation substrates. PTPN13/PTPL1 is widely expressed in the early embryonic stage but mainly in epithelial and nervous tissues in the later stage [15]. In this study, we explored the relationship between the PTPL1 mRNA level and the overall survival time of NSCLC patients based on data from the Kaplan-Meier plotter online database. The subgroup analysis suggested that the overall survival time of lung adenocarcinoma patients was positively correlated with the mRNA level of PTPL1 (HR, 0.49; 95% CI, 0.39-0.63; $P < 0.05$). However, no significant association was found between the level of PTPL1 and the OS time in patients with lung squamous cell carcinoma (HR, 1; 95% CI, 0.79-1.27; $P = 0.99$). However, a study by Han et al involving 91 pairs of cancer and paracancer tissues showed that the expression of PTPL1 was correlated with tumor grade and stage in lung squamous cell carcinoma [32], suggesting the heterogeneity of NSCLC and the limitation of retrospective studies using online data. We need to further explore the correlation between PTPL1 and lung squamous cell carcinoma.

Recent studies have shown that PTPL1 regulates the pathogenesis of many clinical disorders through association with various proteins, such as IκBα, EphrinB, β-catenin, c-Src, insulin receptor substrate 1 (IRS-1), and the growth factor receptor HER2 [17, 18, 29, 33]. PTPL1 can facilitate carcinogenesis by inhibiting Fas-mediated apoptosis or promoting Wnt/β-catenin signaling [19, 20]. In addition, PTPL1 suppresses the development and progression of different tumors by dephosphorylating c-Src or ERK [17, 34]. We demonstrated here that PTPL1 suppresses EMT in NSCLC cells by targeting the TGF-β pathway, consistent with the established tumor-suppressive role of PTPL1 in lung cancer [25].
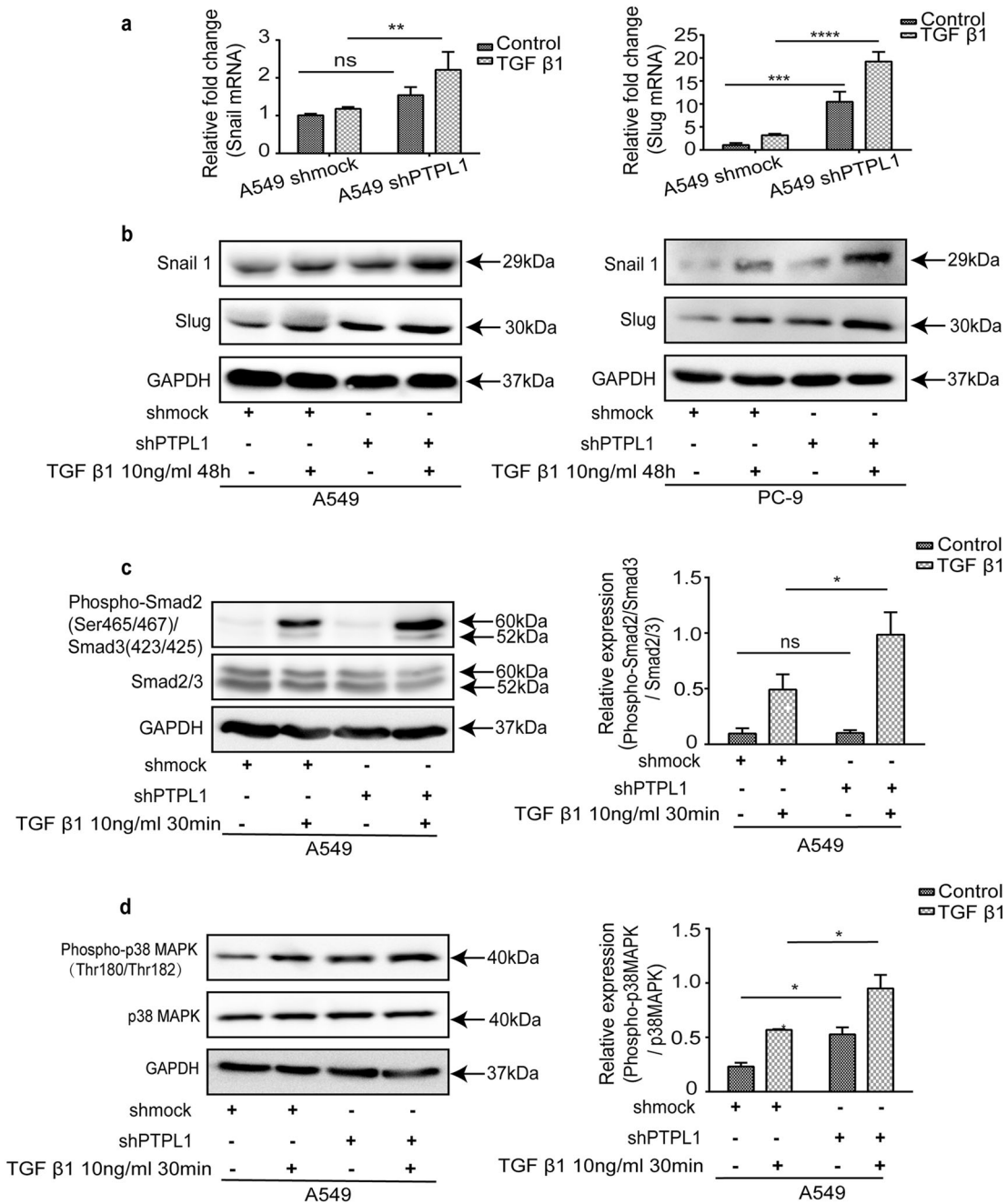
PTPL1 inhibits lung cancer metastasis via P38 MAPK
N Zhu et al.

1285

Fig. 4 PTPL1 silencing upregulates EMT transcription factors via p38 MAPK. a, b NSCLC cells were infected by control lentiviruses (shmock) or those expressing shRNA PTPL1-targeted shRNA, and were further treated with or without TGF-β1. RT-PCR and Western blot were used to measure the expression levels of snail1 and slug (each bar represents the mean ± SEM. **$P < 0.01$, ***$P < 0.001$, ****$P < 0.0001$ vs. the shmock group; ns, non-significant). **c** The protein levels of phospho-Smad2 (Ser465/467)/Smad3 (Ser423/425), Smad2/3 were determined by Western blot analysis using lysates from A549 infected with shmock or shPTPL1 lentiviruses with or without TGF-β1 treatment (each bar represents the mean ± SEM. *$P < 0.05$ vs. the shmock group; ns non-significant). **d** The protein levels of phospho-p38MAPK (Thr180/Tyr182), p38 MAPK were determined by Western blot analysis using lysates from A549 infected with shmock or shPTPL1 lentiviruses with or without TGF-β1 treatment (each bar represents the mean ± SEM. *$P < 0.05$ vs. the shmock group).

The distinct roles of PTPL1 in different tumors can be attributed to varied signaling events that drive carcinogenesis or the context of the signaling network in cells of different tissue origins.

A key inducer of EMT, TGF-β initially binds to TβRII, which subsequently activates downstream signaling mainly through phosphorylation of Smads and p38 MAPK signaling transducers. However, TGF-β signaling is also controlled by a class of protein tyrosine kinases and phosphatases, as exemplified by the documented role of TβRII phosphorylation at several individual tyrosine residues in downstream signaling [35, 36]. Here, we found that PTPL1 dephosphorylates p38MAPK, resulting in repression of noncanonical TGF-β signaling pathways (Fig. 5d). Moreover, we found that PTPL1 knockdown increased the phosphorylation levels of Smad2/3, but unfortunately, this study failed to elucidate the specific molecular mechanism by which PTPL1 regulates Smad2/3 phosphorylation, which will be one of the focuses of our basic research in the future. Collectively, the results of the present study revealed novel mechanisms
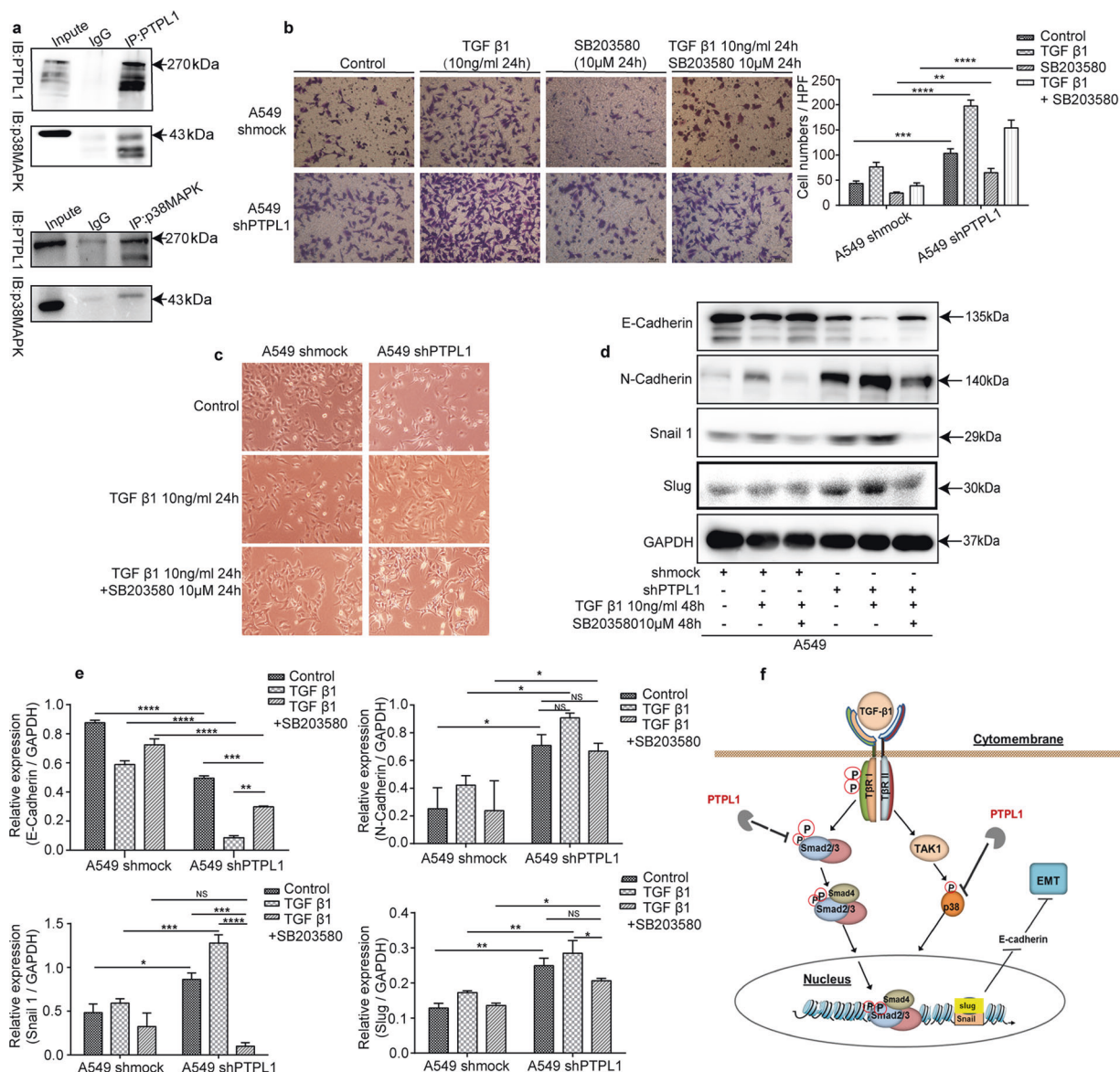
PTPL1 inhibits lung cancer metastasis via P38 MAPK
N Zhu et al.

1286

Fig. 5   PTPL1 inhibits TGF-β signaling and EMT by dephosphorylating p38 MAPK. a Immunoprecipitation using the lysates of A549 cells showing the interaction between PTPL1 and p38 MAPK. **b** Control and PTPL1 knockdown A549 cells were treated with TGF-β1 and/or SB203580, and were subject to Transwell assay for cell invasion (each bar represents the mean ± SEM. **$P < 0.01$, ***$P < 0.001$, ****$P < 0.0001$. ns, non-significant). **c–e** Control and PTPL1 knockdown A549 cells were treated with TGF-β1 and/or SB203580. The morphological changes of the cells were observed by microscope (**c**), and the changes of EMT-related proteins were analyzed by Western blot (**d**, **e**) (each bar represents the mean ± SEM. *$P < 0.05$, **$P < 0.01$, ***$P < 0.001$, ****$P < 0.0001$. ns, non-significant). **f** Schematic diagram for PTPL1 regulation of TGF-β signaling in EMT of NSCLC cells.

underlying the tumor-suppressive role of PTPL1 and the regulation of the noncanonical TGF-β signaling pathway and have implications for prognostic assessment and targeted therapy of metastatic lung cancer.

AUTHOR CONTRIBUTIONS
Authors must indicate their specific contributions to the published work. SQL designed research; NZ and XJZ performed research; HZ, YYZ, JWX, JL, and LD contributed new reagents or analytic tools; PZ, GW and YZZ analyzed data; NZ wrote the paper.

ADDITIONAL INFORMATION
Competing interests: The authors declare no competing interests.

REFERENCES
1. Bray F, Ferlay J, Soerjomataram I, Siegel RL, Torre LA, Jemal A. Global cancer statistics 2018: GLOBOCAN estimates of incidence and mortality worldwide for 36 cancers in 185 countries. CA Cancer J Clin. 2018;68:394–424.
2. Mani SA, Guo W, Liao MJ, Eaton EN, Ayyanan A, Zhou AY, et al. The epithelial-mesenchymal transition generates cells with properties of stem cells. Cell. 2008;133:704–15.
3. Lamouille S, Xu J, Derynck R. Molecular mechanisms of epithelial-mesenchymal transition. Nat Rev Mol Cell Biol. 2014;15:178–96.

PTPL1 inhibits lung cancer metastasis via P38 MAPK
N Zhu et al.

1287

4. Halbleib JM, Nelson WJ. Cadherins in development: cell adhesion, sorting, and tissue morphogenesis. Genes Dev. 2006;20:3199–214.

5. Pastushenko I, Blanpain C. EMT transition states during tumor progression and metastasis. Trends Cell Biol. 2019;29:212–26.

6. Barr S, Thomson S, Buck E, Russo S, Petti F, Sujka-Kwok I, et al. Bypassing cellular EGF receptor dependence through epithelial-to-mesenchymal-like transitions. Clin Exp Metastasis. 2008;25:685–93.

7. De Craene B, Berx G. Regulatory networks defining EMT during cancer initiation and progression. Nat Rev Cancer. 2013;13:97–110.

8. Liu T, Feng XH. Regulation of TGF-beta signalling by protein phosphatases. Biochem J. 2010;430:191–8.

9. Yang H, Wang L, Zhao J, Chen Y, Lei Z, Liu X, et al. TGF-β-activated SMAD3/4 complex transcriptionally upregulates N-cadherin expression in non-small cell lung cancer. Lung Cancer. 2015;87:249–57.

10. Moustakas A, Heldin CH. Signaling networks guiding epithelial-mesenchymal transitions during embryogenesis and cancer progression. Cancer Sci. 2007;98:1512–20.

11. David CJ, Massagué J. Contextual determinants of TGFβ action in development, immunity and cancer. Nat Rev Mol Cell Biol. 2018;19:419–35.

12. Martínez-Estrada OM, Cullerés A, Soriano FX, Peinado H, Bolós V, Martínez FO, et al. The transcription factors Slug and Snail act as repressors of Claudin-1 expression in epithelial cells. Biochem J. 2006;394:449–57.

13. Xu Y, Qin L, Sun T, Wu H, He T, Yang Z, et al. Twist1 promotes breast cancer invasion and metastasis by silencing Foxa1 expression. Oncogene. 2017;36:1157–66.

14. Alonso A, Sasin J, Bottini N, Friedberg I, Friedberg I, Osterman A, et al. Protein tyrosine phosphatases in the human genome. Cell. 2004;117:699–711.

15. Freiss G, Chalbos D. PTPN13/PTPL1: an important regulator of tumor aggressiveness. Anticancer Agents Med Chem. 2011;11:78–88.

16. Dromard M, Bompard G, Glondu-Lassis M, Puech C, Chalbos D, Freiss G. The putative tumor suppressor gene PTPN13/PTPL1 induces apoptosis through insulin receptor substrate-1 dephosphorylation. Cancer Res. 2007;67:6806–13.

17. Glondu-Lassis M, Dromard M, Lacroix-Triki M, Nirdé P, Puech C, Knani D, et al. PTPL1/PTPN13 regulates breast cancer cell aggressiveness through direct inactivation of Src kinase. Cancer Res. 2010;70:5116–26.

18. Sardina JL, López-Ruano G, Prieto-Bermejo R, Sánchez-Sánchez B, Pérez-Fernández A, Sánchez-Abarca LI, et al. PTPN13 regulates cellular signalling and β-catenin function during megakaryocytic differentiation. Biochim Biophys Acta. 2014;1843:2886–99.

19. Gump JM, Staskiewicz L, Morgan MJ, Bamberg A, Riches DW, Thorburn A. Autophagy variation within a cell population determines cell fate through selective degradation of Fap-1. Nat Cell Biol. 2014;16:47–54.

20. Huang W, Bei L, Eklund EA. Fas-associated phosphatase 1 (Fap1) influences β-catenin activity in myeloid progenitor cells expressing the Bcr-abl oncogene. J Biol Chem. 2013;288:12766–76.

21. Han X, Xue L, Zhou L, Gong L, Zhu S, Yao L, et al. The role of PTPN13 in invasion and metastasis of lung squamous cell carcinoma. Exp Mol Pathol. 2013;95:270–5.

22. D'Hondt V, Lacroix-Triki M, Jarlier M, Boissiere-Michot F, Puech C, Coopman P, et al. High PTPN13 expression in high grade serous ovarian carcinoma is associated with a better patient outcome. Oncotarget. 2017;8:95662–73.

23. Wang Z, Shen D, Parsons DW, Bardelli A, Sager J, Szabo S, et al. Mutational analysis of the tyrosine phosphatome in colorectal cancers. Science. 2004;304:1164–6.

24. Yeh SH, Wu DC, Tsai CY, Kuo TJ, Yu WC, Chang YS, et al. Genetic characterization of fas-associated phosphatase-1 as a putative tumor suppressor gene on chromosome 4q21.3 in hepatocellular carcinoma. Clin Cancer Res. 2006;12:1097–108.

25. Scrima M, De Marco C, De Vita F, Fabiani F, Franco R, Pirozzi G, et al. The nonreceptor-type tyrosine phosphatase PTPN13 is a tumor suppressor gene in non-small cell lung cancer. Am J Pathol. 2012;180:1202–14.

26. Xu S, Wang T, Yang Z, Li Y, Li W, Wang T, et al. miR-26a desensitizes non-small cell lung cancer cells to tyrosine kinase inhibitors by targeting PTPN13. Oncotarget. 2016;7:45687–701.

27. Bakin AV, Rinehart C, Tomlinson AK, Arteaga CL. p38 mitogen-activated protein kinase is required for TGFbeta-mediated fibroblastic transdifferentiation and cell migration. J Cell Sci. 2002;115:3193–206.

28. Lee MK, Pardoux C, Hall MC, Lee PS, Warburton D, Qing J, et al. TGF-beta activates Erk MAP kinase signalling through direct phosphorylation of ShcA. EMBO J. 2007;26:3957–67.

29. Zhu JH, Chen R, Yi W, Cantin GT, Fearns C, Yang Y, et al. Protein tyrosine phosphatase PTPN13 negatively regulates Her2/ErbB2 malignant signaling. Oncogene. 2008;27:2525–31.

30. Niu J, Huang YJ, Wang LE, Sturgis EM, Wei Q. Genetic polymorphisms in the PTPN13 gene and risk of squamous cell carcinoma of head and neck. Carcinogenesis. 2009;30:2053–8.

31. Zhan H, Jiang J, Luo C, Sun Q, Ke A, Sun C, et al. Tumour-suppressive role of PTPN13 in hepatocellular carcinoma and its clinical significance. Tumour Biol. 2016;37:9691–8.

32. Han XJ, Xue L, Gong L, Zhu SJ, Yao L, Wang SM, et al. Stat3 inhibits PTPN13 expression in squamous cell lung carcinoma through recruitment of HDAC5. Biomed Res Int. 2013;2013:468963.

33. Welters HJ, Oknianska A, Erdmann KS, Ryffel GU, Morgan NG. The protein tyrosine phosphatase-BL, modulates pancreatic beta-cell proliferation by interaction with the Wnt signalling pathway. J Endocrinol. 2008;197:543–52.

34. Hoover AC, Strand GL, Nowicki PN, Anderson ME, Vermeer PD, Klingelhutz AJ, et al. Impaired PTPN13 phosphatase activity in spontaneous or HPV-induced squamous cell carcinomas potentiates oncogene signaling through the MAP kinase pathway. Oncogene. 2009;28:3960–70.

35. Galliher AJ, Schiemann WP. Src phosphorylates Tyr284 in TGF-beta type II receptor and regulates TGF-beta stimulation of p38 MAPK during breast cancer cell proliferation and invasion. Cancer Res. 2007;67:3752–8.

36. Chen X, Wang H, Liao HJ, Hu W, Gewin L, Mernaugh G, et al. Integrin-mediated type II TGF-β receptor tyrosine dephosphorylation controls SMAD-dependent profibrotic signaling. J Clin Invest. 2014;124:3295–310.